

Journal of Materials Chemistry A

Accepted Manuscript



This is an *Accepted Manuscript*, which has been through the Royal Society of Chemistry peer review process and has been accepted for publication.

Accepted Manuscripts are published online shortly after acceptance, before technical editing, formatting and proof reading. Using this free service, authors can make their results available to the community, in citable form, before we publish the edited article. We will replace this *Accepted Manuscript* with the edited and formatted *Advance Article* as soon as it is available.

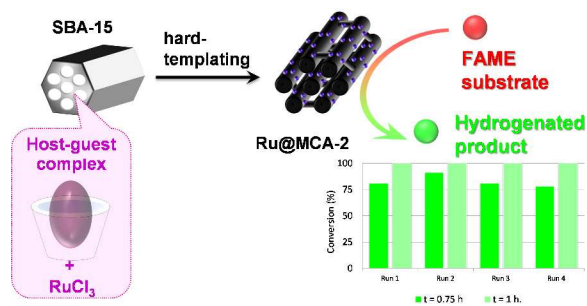
You can find more information about *Accepted Manuscripts* in the [Information for Authors](#).

Please note that technical editing may introduce minor changes to the text and/or graphics, which may alter content. The journal's standard [Terms & Conditions](#) and the [Ethical guidelines](#) still apply. In no event shall the Royal Society of Chemistry be held responsible for any errors or omissions in this *Accepted Manuscript* or any consequences arising from the use of any information it contains.

Table of Contents Entry

A direct novel synthesis of highly uniform dispersed ruthenium nanoparticles over P6mm ordered mesoporous carbon by host/guest complexes

N. Gokulakrishnan,^{a,b,c} G. Peru,^{a,b,c} S. Rio,^{a,b,c} J. F. Blach,^{a,b,c} B. Leger^{a,b,c} D. Grosso,^d E. Monflier,^{a,b,c} and A. Ponchel*^{a,b,c}



A nanocasting strategy to Ru-ordered mesoporous carbon with uniform ruthenium dispersion is demonstrated using a β-cyclodextrin host-guest complex and RuCl₃.

ARTICLE

A direct novel synthesis of highly uniform dispersed ruthenium nanoparticles over P6mm ordered mesoporous carbon by host/guest complexes

Cite this: DOI: 10.1039/x0xx00000x

Received 00th January 2012,
Accepted 00th January 2012

DOI: 10.1039/x0xx00000x

www.rsc.org/

N. Gokulakrishnan,^{a,b,c} G. Peru,^{a,b,c} S. Rio,^{a,b,c} J. F. Blach,^{a,b,c} B. Leger^{a,b,c} D. Grosso,^d E. Monflier,^{a,b,c} and A. Ponchel*^{a,b,c}

We report a novel concept to prepare a highly ordered mesoporous carbon with a uniform dispersion of ruthenium nanoparticles of 1-2 nm size range by a nano-templating method, based on the combined utilization of a β -cyclodextrin host-guest complex and ruthenium trichloride as respective sources of carbon and metal. The composite material synthesized (Ru@MCA-2) through the polymerization and carbonization of these metallo-supramolecular assemblies possesses high surface area and high pore volume after the removal of the silica template and exhibit high catalytic activity in the hydrogenation of unsaturated fatty acid methyl esters. The reusability of this nanoreplicated catalyst is also demonstrated.

Introduction

Since the first synthesis of ordered mesoporous carbons by a hard-templating approach in 1999, these materials have attracted a great deal of attention in a number of high-potential applications including adsorption, sensing, separation, biotechnology and catalysis. Their uses are usually related to their attractive properties such as high surface area, large pore volume, well-tailored pore size, chemical inertness and electrical conducting property.^{1,2} From a practical viewpoint, it is generally accepted that the final properties of ordered mesoporous carbons can be controlled in terms of porosity and hydrophobic/hydrophilic balances, by tuning the textural characteristics of silica templates and selecting appropriate carbon sources. For this purpose, researchers have developed protocols by exploiting various carbon sources ranging from aliphatic to aromatic compounds, such as sucrose, furfuryl alcohol, acenaphthene, anthracene or dihydroxynaphthalene.³⁻⁷

Additionally, for the design of robust and high-efficiency metal supported carbon catalysts, it is important not only to control the size and shape of the nanoparticles, but also take into account the metal-support interactions.⁸⁻⁹ The preparation of well-dispersed metallic nanoparticles on carbons has been described by different techniques, such as ion-exchange or impregnation and the nanocatalysts generally show higher catalytic activities than those obtained on conventional supported systems.¹⁰⁻¹³ However, it is generally assumed that the most important drawback of metal nanoparticles is their tendency to aggregate, especially at high metal contents.

The templating approach based on the use of solid molds offers opportunities for developing novel ordered nanostructures containing metal nanoparticles with a high degree of size control and dispersion.¹⁴ In this context, supramolecular organic templates involving the cooperative assembly of molecules *via* non-covalent interactions can be regarded as promising candidates for the fabrication of tailored metal-incorporated mesoporous carbons. Thus, β -cyclodextrins (cyclic oligosaccharides constituted of seven D-glucopyranose units) are a class of naturally occurring receptors, finding applications in a number of different fields including analytical chemistry, sensing enantiomeric separation, remediation and catalysis.¹⁵⁻¹⁹ Till date, the contribution of cyclodextrins in the elaboration of nanostructured materials and catalysts²⁰⁻²⁴ has been little explored and surprisingly, the possibility of using host-guest complexes with cyclodextrins for the synthesis of structured mesoporous carbons has not yet been investigated. Thus, the pioneering works of Antonietti have shown that worm-like nanoporous silica replicas could be prepared by using cyclodextrins²⁰ and cyclodextrin-based polypseudorotaxanes²¹ as porogen agents by means of a one-pot sol gel process. Pore sizes close to those of the diameters of cyclodextrins (1.5-2 nm) were obtained in the final silica materials. Concerning carbon materials, Han et al. described the synthesis of porous carbon replicas using a sol-gel nanocasting procedure involving the co-condensation of methylated β -CD with tetramethylorthosilicate followed by carbonization and silica removal.²² However, the carbon material resulted in a disordered microporous material with a pore diameter

of ca. 1.6 nm. More recently, the fabrication of mesoporous carbons derived from cyclodextrins with a narrower pore size distribution from 3.2 to 4.2 nm was reported by adding a surfactant (Triton®TX-15) to the silicon alkoxide source.²³

In this paper, we introduce a novel concept to prepare uniformly dispersed metal nanoparticles embedded in the pore walls of an ordered mesoporous carbon by a nanocasting procedure based on the original use of a cyclodextrin host-guest complex and a water-soluble metal salt as respective sources of carbon and metal. Our idea is to take advantage of the unique topologies of cyclodextrin (rigid cyclic structure, large number of hydroxyl groups and ability to form inclusion complexes with molecules of appropriate size and shape) to ensure good dispersion of the metal precursor within the cyclodextrin-based environment in the first step of synthesis, i.e. during the pore filling, and subsequently facilitate the formation of isolated nucleation sites and growth of size-controlled metal clusters during the thermal structuring of the carbon phase. The strategy has been examined through the nanoreplication of SBA-15 using randomly methylated β -cyclodextrin/1-adamantane carboxylic acid (RAMEB/ADAC) as the host-guest system and ruthenium trichloride (RuCl_3) as the metal precursor. 1-adamantane carboxylic acid has been selected for its ability to form stable host-guest complexes with β -CDs. Indeed, the adamantyl group is a highly symmetrical stable structure, which perfectly fits inside the cavity of β -CDs, forming 1:1 inclusion complexes with high association constants (typically in the range of 10^4 – 10^5 M^{-1}).^{25–28} In addition, the presence of the carboxylic acid functionality in the guest molecule is also used to interact favorably with metals. Therefore it is expected that this host-guest concept will facilitate the anchoring of the metal ion to the cyclodextrin (*via* the carboxylic group attached to the adamantane skeleton, itself included in the cyclodextrin cavity) in the first steps of the synthesis and will lead to a good distribution of the metal species in the final carbon replica. For this purpose, we will report that, under well-defined conditions, the utilization of RAMEB/ADAC host-guest assemblies and RuCl_3 allows the synthesis of $P6mm$ ordered mesoporous carbon with uniformly dispersed ruthenium nanoparticles. Furthermore, experiments in the hydrogenation of vegetable oils (methyl oleate) will demonstrate the potential of this material in the field of heterogeneous catalysis.

Experimental

Chemicals

Tetraethylorthosilicate (TEOS), poly(ethylene glycol)-block-poly(propylene glycol)-block-poly(ethylene glycol) (P123; $\text{EO}_{20}\text{PO}_{70}\text{EO}_{20}$; average molecular weight, 5800), hydrochloric acid (HCl, 37 wt. %) and sulfuric acid were purchased from Aldrich. Randomly methylated β -cyclodextrin (RAMEB) with an average substitution of 1.8 methyl groups per cyclodextrin were purchased from Wacker Chemie. Ruthenium chloride hydrate (40–43% of Ru) was purchased from Acros Organics whereas 1-adamantane carboxylic acid was supplied by Aldrich Chemicals. Two different activated carbons used as control support catalysts were selected from commercially available samples. Nuchar®WV-B (denoted AC-WV) was supplied by

MeadWestvaco Corporation, Covington, USA. It was produced from wood and activated with phosphoric acid. Norit®SA-2 denoted (AC-NorA) was produced by Norit (Amersfoort, Netherlands) from peat and steam activated. All other reactants were purchased from Aldrich Chemicals and Acros Organics in their highest purity and used without further purification.

Synthesis of SBA-15

The starting SBA-15 was prepared according to a procedure reported in the literature.²⁹ Briefly, 4 g of P123 was dispersed in 30 g of water by stirring for 3 h. Then, 120 g of a 2 M HCl solution was added to the mixture followed by 2 h stirring at 40 °C and subsequently, 9.0 g of tetraethyl orthosilicate was then added to the homogeneous solution. The mixture was then stirred at 40 °C for 24 h and the resulting gel underwent hydrothermal treatment by heating in an oven at 100 °C for 48 h. The obtained white precipitate was filtered, dried at 100 °C and calcined in a muffle furnace at 550 °C under air. In these experimental conditions, the as-prepared silica has a pore size of ca 8.0 nm and a pore wall thickness of 2.9 nm. The pore wall thickness was calculated according to the formula, $a_0 - (w_d/1.050)$, reported by Kruk et al., where w_d is the BJH pore diameter.³⁰

Preparation of ordered mesoporous ruthenium-carbon material from host-guest complex and RuCl_3

The ruthenium carbon replica has been prepared using a molar composition RAMEB:ADAC:Ru of 5:3:1. The detailed procedure is as follows: 16 mg of RuCl_3 and 18 mg of ADAC were added in 4 ml of water and stirred for 3 h at room temperature. Then 0.6 g of RAMEB was added to the previous mixture and the stirring was continued for further 2 h. Thereafter, 70 mg of H_2SO_4 was added and stirred for 5 minutes, and the resulting mixture was infiltrated into 0.5 g of SBA-15. Subsequently, the mixture underwent polymerization at 60 °C for 24 h. The solid obtained was crushed into powder using mortar and subjected to infiltration again with 10 mg of RuCl_3 , 12 mg of ADAC, 0.4 g of RAMEB and 46 mg of H_2SO_4 under the same conditions to fill the pores completely. After polymerization, the silica-ruthenium-carbon composite was pyrolyzed at 900 °C for 5 h under a nitrogen flow of 150 ml min^{-1} (heating rate of 3 °C min^{-1}). The resulting material was treated with 35% HF to eliminate the silica, filtered by washing with excess amount of water and ethanol and dried at 100 °C. The as-synthesized material is designated as Ru@MCA-2.

Preparation of control carbon materials from RAMEB and RAMEB-ADAC

A ruthenium-free control sample, denoted as MCA-3 has been prepared in a similar manner as that previously described, except that no ruthenium salt was introduced during the procedure. The synthesis of the MCA-3 carbon was carried out by using a mixture of RAMEB to ADAC with a ratio of 5:3 as follows: 16 mg of ADAC and 0.6 g of RAMEB were added together in 4 ml of water and stirred for 2 h at room temperature. After addition of 70 mg of H_2SO_4 , the resulting solution was infiltrated into 0.5 g of SBA-15. Subsequently, the

mixture underwent polymerization at 60 °C for 24 h. The solid is then subjected to infiltration and polymerization again with 11 mg of ADAC, 0.4 g of RAMEB and 46 mg of H₂SO₄ under the same conditions as those previously described. The carbonization was carried out at 900 °C for 5 h under nitrogen flow and the subsequent silica removal was performed by HF etching.

In addition, another ruthenium-free sample has been prepared by replacing the mixture of RAMEB and ADAC with cyclodextrin alone. The synthesis principle was based again on a two consecutive infiltration procedure with 0.6 and 0.4 g of RAMEB, respectively followed by thermo-polymerization at 60°C. The carbonization was carried out at 900 °C for 5 h under nitrogen flow and the subsequent silica removal was performed by HF etching. The synthesized carbon material prepared from RAMEB is designated as MCA-4.

Characterization methods

Small-Angle X-ray Scattering (GISAXS-Rigaku S-max 3000 equipped with a microfocus source $\lambda = 0.154$ nm and a 2D Gabriel type detector placed at 1472 mm from the sample) were used to assess the synthesized material structure. The powder was loaded into a 2 mm in diameter perforation made on a 2 mm thick aluminum plate, before being aligned into the beam. The analysis was performed in vacuum. The d_{100} spacing values were calculated by the formula $d_{100} = 2\pi/q$ and unit cell constants by $a_0 = 2d_{100}/\sqrt{3}$. Transmission electron microscopy (TEM) images were recorded on a TECNAI electron microscope operating at an accelerating voltage of 200 kV. The mesoporous carbon was deposited on a carbon coated copper grid. The carbon nanorod thickness was estimated using Digital Micrograph Software. Nitrogen adsorption isotherms were measured at -196 °C on a Nova 2200 apparatus from Quantachrom Corporation, after having degassed the sample under vacuum at 250 °C. The specific areas were calculated from the Brunauer–Emmett–Teller (BET) equation using P/P_0 values in the 2.5×10^{-2} and 2.0×10^{-1} range and the pore size distributions were obtained from the adsorption branch of the isotherm assuming that the pores are cylindrical using the Barrett–Joyner–Halenda (BJH) method. The total pore volumes were estimated at $P/P_0 = 0.98$ assuming that all the pores were filled with condensed nitrogen in the normal liquid state. The micropore volume is determined by the t-plot method. The percentage of micropore volume in the synthesized materials is calculated as $(\text{Micropore volume}/\text{Total pore volume}) \times 100$. Raman analyses were carried out at room temperature with a Dilor XY-800 confocal micro-Raman spectrometer coupled with a microscope. The spectrum was recorded in back scattering geometry, using the 514.5 nm line of an Ar-Kr laser focused on the sample using a 50 magnification (spot of 2 μm ; power of 20 mW). The Raman cartography was performed using 625 spectra (30 \times 40 μm) at a resolution of 1 μm^2 .

Hydrogenation catalytic tests

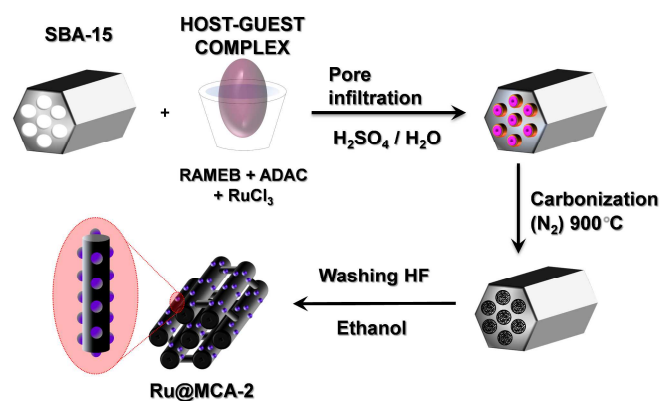
General procedure. The hydrogenation of methyl oleate has been chosen as model reaction and performed as follows: the

stainless steel autoclave was charged with 25 mg of carbon-ruthenium catalyst. 587 mg of methyl oleate (2.07 mmol, 300 equivalents per mol of Ru) was added into the autoclave and hydrogen was introduced at a constant pressure until the desired value is reached (1 to 3 MPa). The mixture was heated to 30 °C and stirred at 1250 rpm. The reaction was monitored by the volume of consumed H₂ and by analysing aliquots of the reaction mixture using a Shimadzu GC-17A gas chromatograph, equipped with a methyl silicone capillary column (30 m \times 0.32 mm) and a flame ionization detector. Each catalytic run was performed in duplicate and the reported results are the average between the two runs.

Reusability. For the recycling procedure, after complete conversion of methyl oleate, the catalyst was recovered by filtration and thoroughly washed with heptane and diethyl ether until complete elimination of the reaction product. After removal of the remaining diethyl ether under vacuum, the solid was reduced under H₂ at 300°C reloaded with methyl oleate and dihydrogen and reused in hydrogenation as described above.

Results and discussion

Scheme 1 depicts the synthesis of the ruthenium carbon replica, Ru@MCA-2, prepared from a host-guest assembly acting metal carrier and carbon source. The synthesis procedure involves the filling of the silica pores with a host-guest solution formed between the methylated cyclodextrin and ruthenium adamantane followed by a polymerization step with sulfuric acid at 60°C. The resultant product is carbonized at 900°C in an inert atmosphere and finally treated by HF to remove the silica hard-template.



Scheme 1 Schematic illustration of the synthesis of Ru@MCA-2 by hard templating from host/guest complexes

The structure and crystallinity of the Ru@MCA-2 material has been elucidated by the analysis of the SAXS pattern, which shows an intense low-angle diffraction peak and two weak peaks, assigned to the (100), (110) and (200) reflections of a 2D-hexagonal P6mm structure, respectively (Figure 1). These features are indicative of the fact that the ruthenium-carbon replica preserves an ordered structure by retaining the hexagonal symmetry of the SBA-15 silica template. It is worthy

to note that the SAXS patterns obtained from the control carbon materials, i.e. MCA-3 (RAMEB + ADAC) and MCA-4 (RAMEB) exhibit similar reflection planes, corroborating again that the carbons are negative replicas of the SBA-15 without any marginal structural disorder. These results are consistent with the stabilization of a CMK-3 type mesoporous carbon whose structure is composed of carbon nanorods arranged in a hexagonal pattern rigidly interconnected therebetween.⁶

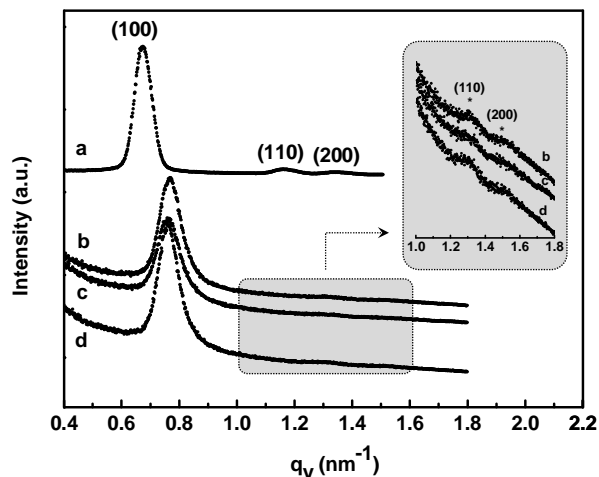


Figure 1 SAXS pattern of the synthesized materials: (a) SBA-15, (b) Ru@MCA-2, (c) MCA-3 and (d) MCA-4.

The unit cell parameters for the synthesized silica and carbon materials calculated from the d_{100} spacing values are provided in Table 1. It can be observed that the unit cell constants are very similar for the three carbon materials with a value of 9.5–9.6 nm, indicating that the polymerization of RAMEB with or without adamantyl guests trapped inside the cavity of the β -cyclodextrin does not result in any appreciable change in the ordered structure of the carbon replicas after carbonization and silica removal. Thus, the use of free and complexed cyclodextrins as carbon sources is expected to lead to relatively well-ordered structures of carbon nanorods because the cyclodextrins molecules would easily form a condensed structure during the gelation step due to their ability to pack in head-to-head arrangements (channel structure).²⁴ These results suggest that the cyclodextrins get polymerized by preserving the guest molecules inside the cavities, which are later carbonized at higher temperatures. Interestingly, the process of carbon formation involving the use of supramolecular assemblies can be successfully applied to the case of metal-carbon composites *via* the use of a suitable metal precursor, as evidenced by the Ru@MCA-2 sample synthesized by inclusion complexation of RAMEB and 1-adamantane carboxylic acid in the presence of ruthenium trichloride. In addition, a comparison of the unit cell parameters for the carbon replicas shows that the values are 12 % lower than that for the SBA-15 template, which indicates a slight decrease in the volume of channels within the silica framework and structural shrinkage of the materials after thermal treatment at 900°C.²⁶

Table 1 Structural and textural properties of the mesoporous carbons prepared from RAMEB and starting silica hard- template

Sample	d_{100} (nm) ^a	a_0 (nm) ^b	S_{BET} (m ² g ⁻¹) ^c	V_p (cm ³ g ⁻¹) ^d		% ^f	D_p (nm) ^g
				V_{meso}	V_{micro} ^e		
SBA-15	9.3	10.8	771	1.016	0.005	0.49	7.9
Ru@MCA-2	8.2	9.5	945	0.899	0.041	4.36	3.8
MCA-3	8.3	9.6	959	1.006	0.034	3.37	4.2
MCA-4	8.2	9.5	945	1.103	0.027	2.37	4.2

^a d-spacing calculated on the basis of the following formulas $n\lambda = 2d_{100}\sin\theta$ and $d_{100} = 2\pi/q$. ^b unit cell constant calculated by the equation $a_0 = 2d_{100}/\sqrt{3}$. ^c specific surface area calculated from the Brunauer-Emmet-Teller equation in the P/P_0 range of 0.025–0.20. ^d determined at $P/P_0 = 0.98$. ^e total pore volume estimated at $P/P_0 = 0.98$. ^f micropore volume determined by the t-plot method. ^g percentage of micropore calculated as the ratio of micropore volume to total pore volume $\times 100$. ^h calculated by the Barrett-Joyner-Halenda method from the adsorption branch of the isotherm assuming cylindrical.

As can be seen from the Figure 2, the N₂ adsorption-desorption isotherms for all samples are characteristic of a type IV isotherm of mesoporous materials with a hysteresis loop featuring the capillary condensation at intermediate P/P_0 pressures: ~ 0.55 – 0.85 for SBA-15 *vs* ~ 0.4 – 0.85 for the synthesized carbon materials. It is apparent, from the pore size distributions (PSD) that only one type of pores in the carbon replicas is distinguished, i.e. the pores formed by removal of the silica wall and confined between the hexagonally packed carbon rods. This confirms that the resulting carbons derived from RAMEB are inverse replicas of the silica framework by maintaining a high degree of pore-size uniformity with, in addition, a high surface area and pore volume (Table 1). Thus, it can be noted that the textural features of MCA-3 (RAMEB + ADAC) are almost the same as those of MCA-4 (RAMEB), in terms of specific surface area (~ 940 – 960 m² g⁻¹), total pore volume (~ 1.0 – 1.1 cm³ g⁻¹) and pore diameter (4.2 nm). It is remarkable that the overall contribution of micropores is quite low in all these materials ($< 5\%$). This result could be related to the fact that RAMEB is an oligosaccharide with a relatively low oxygen-to-carbon ratio of 0.6 (molecular formula: C₅₅H₉₅O₃₅) and that its conversion into carbon by polymerization and carbonization at 900°C does not develop large amounts of micropores within the carbon nanorods. Indeed, it is generally accepted that CMK-3 type materials produced from the common precursor sucrose ($O/C = 0.9$)[†] lead to the formation of additional micropores and disordered carbon networks, responsible for the increase in the specific surface areas (~ 1300 – 1500 m² g⁻¹).^{1–3} Finally, the features obtained in this work can be viewed as an indication that relatively ordered carbon structures can be directly obtained from cyclodextrin inclusion complexes because the guest adamantane molecules trapped in the host cavity of RAMEB would not significantly affect the process of carbon nanorod formation. However, in the case of Ru@MCA-2, a little alteration in the porous structure is encountered and this can be attributed to the incorporation of ruthenium nanoparticles within the carbon matrix.

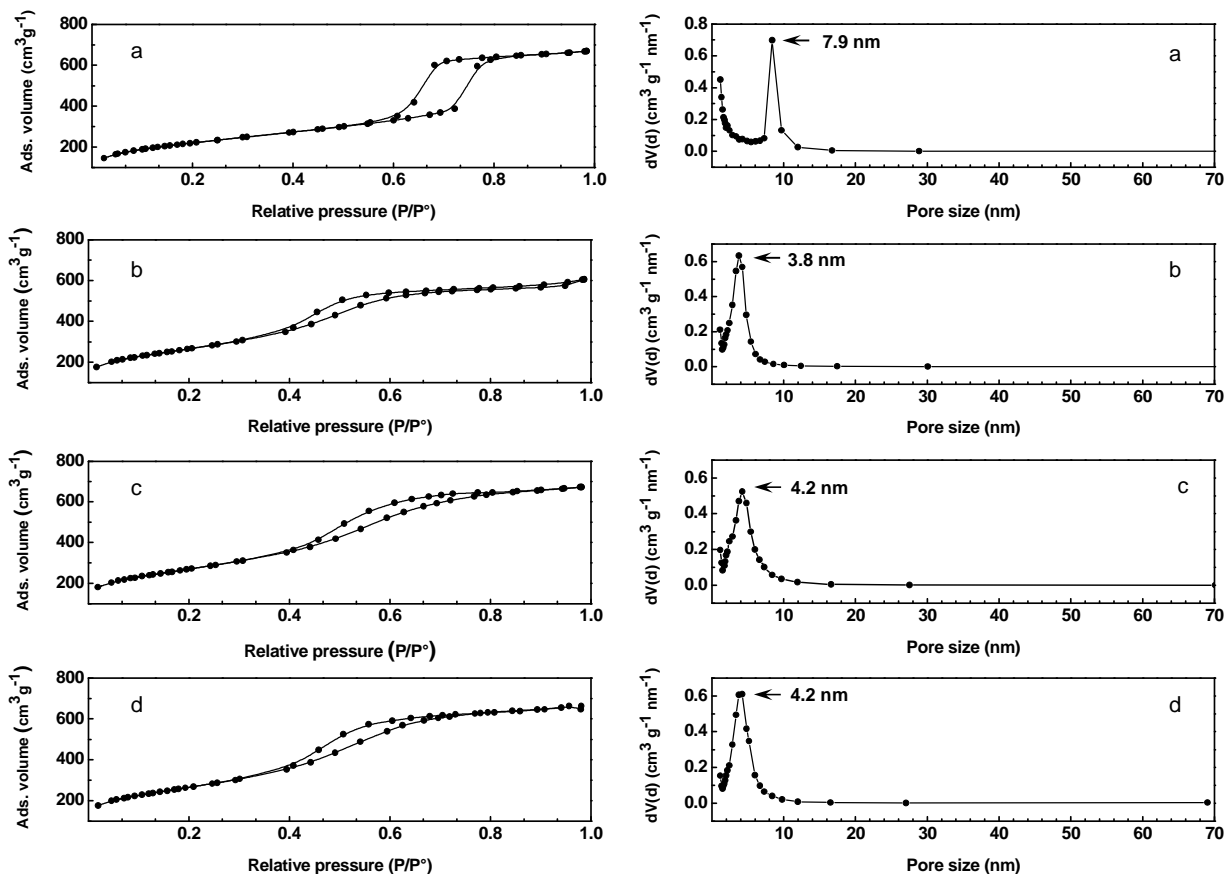


Figure 2. N_2 adsorption-desorption isotherms of the synthesized materials and their corresponding BJH pore size distributions: (a) SBA-15, (b) Ru@MCA-2, (c) MCA-3 and (d) MCA-4.

In addition, we observe that the pore sizes of the carbon replicas are larger by approximately 0.5–0.9 nm than that of the pore wall thickness of the starting SBA-15 (3.3 nm). The deviation may be related to the aforementioned structural shrinkage during the carbonization process. The structural characterization of the synthesized carbon materials prepared from host-guest assemblies has been further explored by TEM analysis (Figure 3). Figures 3a and 3b show the TEM images of the MCA-3 sample (RAMEB + ADAC) viewed perpendicular and parallel to the carbon rods, respectively. Thus, we observe that MCA-3 forms a periodic arrangement of interconnected filled carbon nanorods, with a parallel alignment between mesoporous channels on a long range order, i.e. more than 600 nm long (Figure 3a) and a honeycomb structure (Figure 3b). This observation corroborates the fact that MCA-3 has a 2D-hexagonal structure similar to that in a CMK-3 structure ($P6mm$). The structure and metal dispersion of the Ru@MCA-2 sample was also verified by TEM measurements (Figures 3c to 3g). Like MCA-3, the Ru@MCA-2 sample exhibits a uniform

array of mesopores with a long range order. The average carbon rod thickness is estimated to be ca. 6 nm (Figure 3e), which is somewhat smaller than that of the pore diameter of the SBA-15 silica template due to the shrinkage during the thermal treatment. In addition, it can be seen that, for this composite material prepared by exploiting the complexation interactions of β -cyclodextrin and the adamantane derivative, ruthenium particles with an average size of ca. 1.5 nm are uniformly dispersed over the carbon nanorods. As shown in Figure 3h, the histogram displays a narrow-size distribution, with more than 95 % of the nanoparticles between 1 and 2 nm in size. No agglomeration of nanoparticles was observed. It can be further noted that Ru@MCA-2 has also been analyzed by wide angle XRD to support the absence of large aggregates in the sample (Figure S1, Supporting Information). Thus, no reflection peaks of ruthenium in the form of metallic and/or oxide phase emerge from the XRD pattern, further indicating that ruthenium forms very small particles within the carbon matrix, which cannot be detected by wide angle XRD analysis.^{31,32}

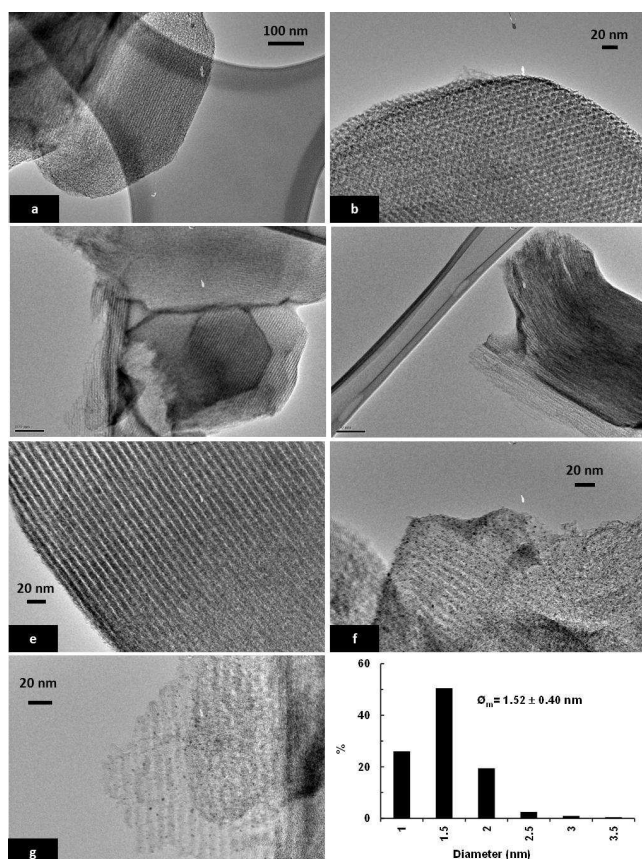


Figure 3 TEM images of the carbon materials prepared from cyclodextrin inclusion complexes at different magnifications: (a) MCA-3 at 100 nm; (b) MCA-3 at 20 nm; (c) and (d) Ru@MCA-2 at 100 nm; (e), (f), (g) Ru@MCA-2 at 20 nm and (h) the corresponding particle size distribution of Ru@MCA-2 obtained from the measurement of ca. 200 particles

Taken together, these results suggest that the synthesis strategy presented in this study enables to distribute homogeneously the ruthenium ions within the cyclodextrin-adamantane network (itself confined to the pores of the silica template) and maintain the ruthenium dispersion in the subsequent steps of polymerization, carbonization and HF etching. In addition, it is worth noting that the ruthenium content has been determined in two different batches of Ru@MCA-2 samples by elemental analysis (SCA, CNRS) and the metal loading was 2.7 ± 0.03 wt. %. Interestingly, this value is relatively close to that which would be expected by considering the complete transformation of both organic precursors into carbon without loss of metal (~ 2.1 wt. %). These results are further evidence of the efficiency of the synthesis method that allows easy control of the metal loading and size of the metallic nanoparticles in the final structure.

The synthesized mesoporous carbon materials were also investigated by Raman spectroscopy to study their graphitic character (Figure 4a and Figure S2, Supporting Information). All Raman spectra reveal a set of two bands at 1310 and 1590 cm^{-1} , assigned to defects or (D band) and graphitic structures (G band) in carbon materials, respectively.

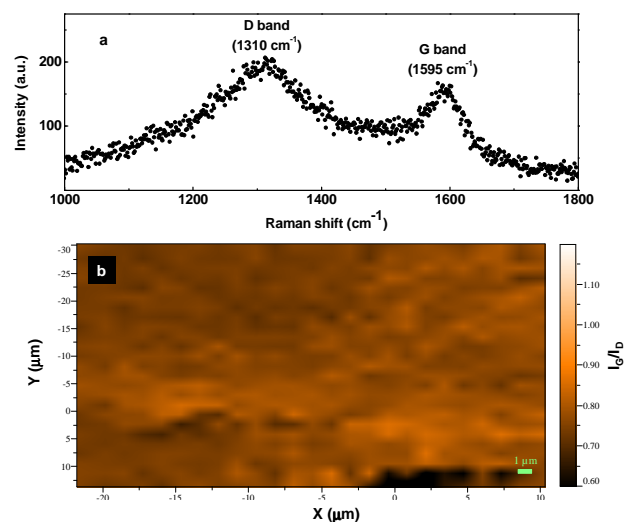


Figure 4 (a) Raman spectrum of the Ru@MCA-2 sample; (b) Raman cartography calculated from the intensity ratio of IG to ID at 1595 and 1310 cm^{-1} , respectively (625 pixels).

The formation of some graphitic domains within the carbon networks prepared from cyclodextrins and inclusion complexes is evidenced by the presence of the narrow band ascribed to the stretching vibration modes of C=C bonds of typical graphite layers at 1590 cm^{-1} . The other band at 1300 cm^{-1} is associated with the vibration of carbon atoms in plane terminations of disordered graphite. The I_G/I_D ratio of Ru@MCA-2, MCA-3 and MCA-4 is calculated to be 0.83, 0.84 and 0.87, respectively and these values indicate the relatively good graphitic nature of the carbon framework compared to other commercial carbons⁵ (activated carbon, carbon black) and synthesized ordered mesoporous carbon materials, such as CMK-3,³³ CMT-1,³⁴ CMK-3-MPc³⁵ and OMCs-SGW.³⁶ A two-dimensional Raman cartography ($30 \times 40 \mu\text{m}$) at a resolution of $1 \mu\text{m}^2$ was further performed to establish the spatial distribution of the two bands by calculating the ratio of the peak heights of 1590 to 1310 cm^{-1} . The result of the mapping recorded on Ru@MCA-2 is outlined on Figure 4b and allows highlighting the homogeneity of this sample on a larger scale than that usually studied with the standard Raman microscope measurement. Thus, we observe that the I_G/I_D ratio is mostly in the range of 0.75 to 0.90 and that ca. 3 % of the pixels are less than or equal to the threshold value of 0.6.

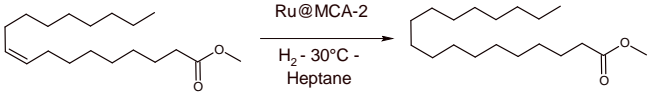
To illustrate the interest of the strategy of synthesis, the activity of Ru@MCA-2 was investigated in the hydrogenation of methyl oleate, chosen as a model molecule of unsaturated fatty acid methyl esters (Table 2). Hydrogenation of fatty oils and fatty acid methyl esters is one of the most important processes in edible oil and oleochemical industries in order to make the products more resistant against air autoxidation, thermal decomposition, and other reactions that affect the flavor. Catalytic tests have been performed in heptane at 30°C under various pressures of H_2 ranging from 1 to 3 MPa and with a ratio of substrate to ruthenium of 300. The reaction kinetic is

monitored by gas chromatography (procedure in the experimental section).

For comparison, the results obtained with two control ruthenium carbon-supported catalysts containing the same metal loading than that of Ru@MCA-2 (2.7 wt. % Ru) have been added. Briefly, these control materials were prepared by wet impregnation of RuCl₃ followed by calcination under air at 250°C and reduction at 300°C under H₂ (20 vol. % in N₂). Two commercial activated carbons were selected to support the ruthenium active phase, i.e., AC-WV (1690 m² g⁻¹) and AC-NorA (1207 m² g⁻¹). The corresponding textural parameters and surface titration are given in Table S1 (Supporting Information). Compared to AC-NorA, it is shown that AC-WV exhibits a higher surface area (1690 vs 1207 m² g⁻¹), a larger average pore size (3.1 vs 2.4 nm) and a lower percentage of microporosity (41 vs 60 %).

The results presented in Table 2 reveal that the activity of Ru@MCA-2 is highly dependent on the pressure of H₂, the higher the pressure, the higher the activity. Thus, the highest turnover frequency of the Ru@MCA-2 catalyst for the hydrogenation of methyl oleate reaches ca. 400 h⁻¹ at 3 MPa and notably this value is 4 times higher than that of control Ru/AC-WV. As the conversion of methyl oleate was negligible in the presence of Ru/AC-NorA after 3 hours reaction, we do not extend the time to complete the reaction. From these results, it can be assumed that the Ru@MCA-2 catalyst prepared by the cyclodextrin approach has more exposed metallic surface thanks to a high dispersion of small Ru nanoparticles whereas the carbon-supported ruthenium catalysts prepared by wet impregnation can more easily undergo aggregation during the thermal treatments and reaction course.

Table 2 Catalytic performances of methyl oleate hydrogenation catalyzed by Ru catalysts



Sample	H ₂ (MPa)	Conv. (%) ^a	Time (h) ^b	TOF (h ⁻¹) ^c
Ru@MCA-2	1	5 ^d	-	-
Ru@MCA-2	2	15 ^d	18	16.7
Ru@MCA-2	3	74	1	400
Ru/AC-WV	3	20	3	100
Ru/AC-NorA	3	4 ^d	-	-

^a Conversion after 0.5 h. ^b 100 % conversion. ^c Turnover frequency defined as the number of mol of substrate per mol of ruthenium per h. ^d Conversion after 3 h. Reaction conditions: Catalyst (2.7 wt. % Ru), 25 mg; Ru, 6.9 μmol; Methyl oleate, 2.08 mmol; Substrate/Ru (mol/mol), 300; Heptane, 10 g; H₂, 1- 3 MPa; Stirring rate, 1250 rpm; Temperature, 30°C.

The catalytic results also suggest that Ru@MCA-2 has the advantage to combine a high surface area and uniform pore size within the hexagonal arrangement of the carbon nanorods. These textural features are important factors for the diffusion of

the bulky hydrophobic substrate, i.e. methyl oleate, into the porous network of the catalyst prepared by hard-templating.^{3,37,38} In contrast, the extremely low activity obtained Ru/AC-NorA, can be related to the predominant microporous structure of the activated carbon that provides steric hindrance to the long-chain fatty acid methyl ester molecules and prevents their accessibility onto metal active sites. Finally, the reusability of Ru@MCA-2 has been evaluated on methyl oleate at 3 MPa H₂ and 30°C (Figure 5). We observe that the Ru@MCA-2 catalyst is stable and reusable under the reaction conditions, preserving its activity after 4 consecutive runs.

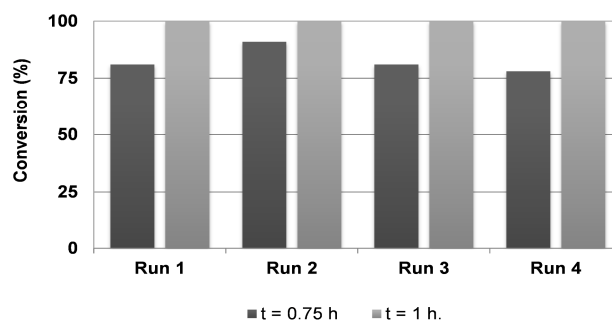


Figure 5 Reusability of the catalytic system in the hydrogenation of methyl oleate. Reaction conditions: Catalyst Ru@MCA-2 (2.7 wt. % Ru); Methyl oleate /Ru (mol/mol), 300; Heptane, 10 g; H₂, 3 MPa; Stirring rate, 1250 rpm; Temperature, 30°C.

Conclusions

In conclusion, we have described a one-pot method for the preparation of a P6mm ordered mesoporous carbon having uniform ruthenium nanoparticles ranging from 1 to 2 nm. The specificity of the method was based on the ability of methylated β-cyclodextrin to act as both a polymerizable carbon source and a host molecule for favoring the inclusion of a carboxylic acid derivative and the dispersion of the ruthenium precursor during the pore filling and gelation steps. The ruthenium dispersion could be maintained without any sign of aggregation after the thermal structuring of the carbon phase at 900°C and silica removal. Finally, the nanocasting strategy involving the direct use of host-guest complexes could contribute to provide a new generation of robust catalysts with high metal dispersions and stability while ensuring the stabilization of ordered mesoporous carbons of high specific surface areas and pore volumes. These features are known to be key factors to ensure accessibility to the active sites and efficient mass transports in heterogeneous catalytic processes.

Acknowledgements

Dr. N. Gokulakrishnan is thankful for financial support by the Institut de Recherche en Environnement Industriel. The TEM facility in Lille (France) is supported by the Conseil Regional du Nord-Pas de Calais and the European Regional Development Fund (ERDF). The SAXS facility in the Collège

de France is supported by the CBRSn, the UPMC and Cnano Ile de France. The authors gratefully acknowledge the National Agency of Research (CYCLOMAT N° ANR-11-NANO-005) for funding.

Notes and references

^a Univ Lille Nord de France, F-59000 Lille, France.

^b UArtois, Unité de Catalyse et Chimie du Solide (UCCS), Faculté des Sciences Jean Perrin, Rue Jean Souvraz, F-62307 Lens, France.

^c CNRS, UMR 8181, F-59650 Villeneuve d'Ascq, France.

^d Laboratoire Chimie de la Matière Condensée de Paris, UMR-7574, Collège de France, 11, place Marcelin Berthelot, 75231 Paris, France.

† CMK-3 was prepared from sucrose (molecular formula: C₁₂H₂₂O₁₁) by a two consecutive infiltration procedure, involving a thermopolymerization reaction at 100 and 160 °C. The carbonization was carried out at 900 °C for 5 h under nitrogen flow and the silica removal was performed by HF etching [6].

Electronic Supplementary Information (ESI) available: [Wide angle XRD pattern of Ru@MCA-2 sample (Figure S1). Raman spectra of the carbon materials obtained from host guest complexes (RAMEB+ADAC) and cyclodextrins (RAMEB) (Figure S2). Main characteristics of the activated carbons used as supports for the preparation by impregnation of the control Ru/C catalysts (Table S1)]. See DOI: 10.1039/b000000x/

- R. Ryoo, S. H. Joo and S. Jun, *J. Phys. Chem. B*, 1999, **103**, 7743.
- T. Y. Ma, L. Liu and Y. Z. Yuan, *Chem. Soc. Rev.*, 2013, **42**, 3977.
- N. Gokulakrishnan, B. Léger, C. Lancelot, S. Fourmentin, D. Grosso, E. Monflier and A. Ponchel, *Carbon*, 2011, **49**, 1290.
- J. Lee, J. Kim and T. Hyeon, *Adv. Mater.*, 2006, **18**, 2073.
- T. W. Kim, I. S. Park and R. Ryoo, *Angew. Chem. Int. Ed.*, 2003, **42**, 4375.
- S. Jun, S. H. Joo, R. Ryoo, M. Kruk, M. Jaroniec, Z. Liu, T. Ohsuna and O. Terasaki, *J. Am. Chem. Soc.*, 2000, **122**, 10712.
- C. H. Kim, D. K. Lee and T. J. Pinnavaia, *Langmuir*, 2004, **20**, 5157.
- R. Narayanan and M. A. El-Sayed, *Langmuir*, 2005, **21**, 2027.
- R. White, R. Luque, V. L. Budarin, J. H. Clark and D. J. Macquarrie, *Chem. Soc. Rev.*, 2009, **38**, 481.
- S. Ikeda, S. Ishino, T. Harada, N. Okamoto, T. Sakata, H. Mori, S. Kuwabata, T. Torimoto and M. Matsumura, *Angew. Chem. Int. Ed.*, 2006, **118**, 7221.
- R. Narayanan and M. A. El-Sayed, *J. Catal.*, 2005, **234**, 348.
- J. M. Nadgeri, M. M. Telkar and C. V. Rode, *Catal. Commun.*, 2008, **9**, 441.
- R. Luque, J. H. Clark, K. Yoshida and P. L. Gai, *Chem. Commun.*, 2009, 5305.
- Y. Li, G. Lan, H. Wang, H. Tang, X. Yan and H. Liu, *Catal. Commun.*, 2012, **20**, 29.
- J. Szejtli, *Chem. Rev.*, 1998, **98**, 1743.
- R. Breslow and S. D. Dong, *Chem. Rev.*, 1998, **98**, 1997.
- F. Hapiot, S. Tilloy and E. Monflier, *Chem. Rev.*, 2006, **106**, 767.
- F. Hapiot, A. Ponchel, S. Tilloy and E. Monflier, *C. R. Chimie*, 2011, **14**, 149.
- L. X. Song, L. Bai, X. M. Xu, J. H. He and S. Z. Pan, *Coord. Chem. Rev.*, 2009, **253**, 1276.
- S. Polarz, B. Smarsly, L. Bronstein and M. Antonietti, *Angew. Chem. Int. Ed.*, 2001, **40**, 4417.
- B. H. and M. Antonietti, *Chem. Mater.*, 2002, **14**, 3477.
- B. H. Han, W. Zhou, and A. Sayari, *J. Am. Chem. Soc.*, 2003, **125**, 3444.
- W. Shen, X. Yang, Q. Guo, Y. Liu, Y. Song, Z. Han, Q. Sun and J. Cheng, *Mater. Lett.*, 2006, **60**, 3517.
- H. C. Wang, B. L. Li, J. T. Li, P. Lin, X. B. Bian, J. Li, B. Zhang and Z. X. Wan, *Appl. Surf. Sci.*, 2011, **257**, 4325.
- W. C. Cromwell, K. Bystrom and M. R. Eftink, *J. Phys. Chem.*, 1985, **89**, 326.
- R. I. Gelb and L. M. Schwartz, *J. Incl. Phenom. Mol. Recogn. Chem.*, 1989, **7**, 537.
- R. Palepu and V. C. Reinsborough, *Aust. J. Chem.*, 1990, **43**, 2119.
- E. S. Kwak and F. A. Gomez, *Chromatographia*, 1996, **43**, 659.
- M. Hartmann and A. Vinu, *Langmuir*, 2002, **18**, 8010.
- M. Kruk, M. Jaroniec, Y. Sakamoto, O. Terasaki, R. Ryoo and C. H. Ko, *J. Phys. Chem. B*, 2000, **104**, 292.
- R. W. G. Wyckoff, In *Crystal Structures*. Second Edition, Interscience Publishers, Vol. 1, pp. 7–83, New York, 1963.
- J. Haines, J. M. Léger, O. Schulte and S. Hull, *Acta Crystallogr. Sect. B*, 1997, **53**, 880.
- L. Shen, E. Uchaker, C. Yuan, P. Nie, M. Zhang, X. Zhang and G. Cao, *ACS Appl. Mater. Interfaces*, 2012, **4**, 2985.
- Y. Lo, S. J. Huang, W. H. Chen, Y. R. Peng, C. T. Kuo and S. B. Liu, *Thin Solid Films*, 2006, **498**, 193.
- K. T. Lee, X. Ji, M. Rault and L. F. Nazar, *Angew. Chem. Int. Ed.*, 2009, **48**, 5661.
- Z. Wu, Y. Yang, D. Gu, Y. Zhat, D. Feng, Q. Li, B. Tu, P. A. Webley and D. Y. Zhao, *Top. Catal.*, 2009, **52**, 12.
- N. Kania, B. Léger, S. Fourmentin, E. Monflier and A. Ponchel, *Chem. Eur. J.*, 2010, **16**, 6138.
- N. Kania, N. Gokulakrishnan, B. Léger, B., S. Fourmentin, E. Monflier and A. Ponchel, *J. Catal.*, 2011, **278**, 208.